Novel Target Fabrication Using 3D Printing Developed at University of Michigan

Sallee R Klein[1], Michael Deininger[2], Robb S Gillespie[1], Carlos A Di Stefano[1], Michael J MacDonald[1], Mario J-E Manuel[1], Rachel P Young[1], Carolyn C Kuranz[1], Paul A Keiter[1] and R Paul Drake[1]

[1]Department of Atmospheric, Oceanic and Space Sciences, University of Michigan, Ann Arbor MI

[2]Medical Innovations Center, University of Michigan, Ann Arbor MI

E-mail: `salleer@umich.edu`

Abstract. The University of Michigan has been fabricating targets for high-energy-density experiments for the past decade. We utilize the technique of machined acrylic bodies and mating components acting as constraints to build repeatable targets. Combining 3D printing with traditional machining, we are able to take advantage of the very best part of both aspects of manufacturing. Here we present several recent campaigns to act as showcase and introduction of our techniques and our experience with 3D printing, effecting how we utilize 3D printing in our target builds.

1. Introduction

Target fabrication is a crucial aspect of high-energy-density-physics. To enable physicist to compare results from different targets within an experimental campaign, designing and building repeatable targets is fundamental to obtaining meaningful data. Finding better ways to build targets with ever challenging geometries can be difficult. At the University of Michigan we have been designing targets comprised of acrylic outer structures that facilitate precisely built targets. Our acrylic structures enable us to build the majority of our targets by hand, using no mechanism. This technique generates targets as repeatable as our machining, reducing target to target variation substantially. Often the target design is too complex to machine as one piece. We then fabricate the acrylic outer structure in two pieces that mate in an unique configuration constraining individual components in precise orientations. In this manner, targets cannot be assembled incorrectly because the parts simply won't connect to one another. Over the years this method of building targets has been quite successful. But recently we have had to cope with the demands of shooting at smaller facilities where shot times extend over weeks, requiring targets that can number well over 100. Traditionally machining this many targets is not practical. Not only can the sheer number of targets become daunting, but designs have become ever more complex. Some of the designs required are simply not possible to machine in a traditional manner. Born from the overwhelming amount of targets needed and the increasing sophistication with target designs, we began to test how 3D printing could be of benefit to us and the target fabrication community in general.

We will begin by discussing the motivation for implementing acrylic structures for our targets, serving as explanation for why this element to our target builds has become such an integral part of our fabrication process. We will then detail several campaigns in which we implemented 3D printing into our targets and how that has changed the way in which we design outer structures of targets to adjust to the limitations that come with 3D printing on this scale. We conclude by explaining how we were able combine 3D printing and traditional mating in the most precise and efficient manner.

Our research focuses on laboratory astrophysics. This includes, but is certainly not limited to, instabilities such as RayleighTaylor, Richtmyer-Meshkov and KelvinHelmholtz. We also study radiative shock, magnetized plasmas, plasma jets, reverse radiative shock, hot electrons, Thomson scattering, x-ray fluorescence and plasma sheet experiments, to name a few. We preform these experiments at several laser facilities around the United States. Typically, we run experiments at OMEGA, located at the Laboratory for Laser Energetics (LLE) at the University of Rochester, but we often use smaller facilities such as Titan at Lawrence Livermore National Laboratory (LLNL) and Trident at Los Alamos National Laboratory (LANL).

An example of a typical experiment shot on Omega-60 is our radiative shock campaign. For this campaign the targets have small polyimide tubes, 625 μm outside diameter (OD) with a wall thickness of 25 μm, that is pressurized with xenon gas. This polyimide shock tube is connected to a Tygon gas fill tube with a stainless steel hypo-tube, whose ends are inserted into the Tygon fill tube and the polyimide shock tube. This connection is sealed with UV cured glue. With the Tygon gas fill line attached, the tiny polyimide shock tube has a substantial amount of weight added to it. If the shock tube were to bend from the weight of the gas fill line it would be out of the field of view in the experiment. Also, any damage to the walls of the tube will cause a loss of pressure, therefore eliminating the possibility of obtaining any data. In the original radiative shock target (Figure 1, left) the gas fill tube had to be glued to the stalk to help support the shock tube in an attempt to mitigate any damage to the shock tube from the weight of the gas fill tube and the chances that this shock tube will get bent during handling. Another potential hazard was that the stainless steel hypo-tube needed to be bent within the gas fill line further attempting to alleviate stress on the tiny polyimide shock tube. This makes handling the target, such as adding additional components, taking it in and out of its case, leak testing, travel, gas fill and loading into the target chamber, precarious. This was a difficult task that did not always leave the tube in the intended position for the experiment. Therefore, the targets were not as repeatable from target to target, with respect to the shock tube position, and more targets had to be built to compensate for damaged ones.

This target design is a particularly good illustration of how fabricating targets using acrylic structures offers many benefits. The most immediate benefit is that they are less expensive. Gold shielding in the shape of wedges can be cut from gold foil and placed only in the radiography views, therefore eliminating the need for the entire cone to be made of gold. The acrylic cone acts as scaffolding to glue the wedges onto. Since the cone is transparent, it can be align in the target chamber using micro-dots or circular reticles. Stalk flags are unnecessary. The stalk hole is directly drilled into the acrylic body at the specific angles needed for the experiment. The tungsten-carbide stalk is simply inserted into the stalk hole, and requires no special equipment to stalk. With this method of stalking, target to target variability in stalk angles are better than can be measured. Because this particular target had a gas-filled tube, supporting this tube was crucial, as mentioned above. To add complexity, the tube in the final two radiative shock campaigns had an elliptical cross section. The orientation of the tube was vital, therefore, for the final two campaigns in this series of radiative shock experiments, the design was modified by adding an acrylic cap to the back of the cone that locked into place in a unique position.[1] The tube was then threaded through the elliptical hole in the rear of the cap and attached within the elliptical hole in the cone. The cap simply clipped onto the back of the cone in an

unique orientation, constraining the elliptical tube into the correct orientation. With the cap snuggly clipped onto the cone the orientation of the major and minor axis of the elliptical tube were in the correct diagnostic viewing windows as needed for the experiment. Figure 1 depicts the completed target on the right. The bare tube can be seen through the diagnostic windows. These windows also provided a surface from which to attach fiducials. In this case, we placed a fiducial grid in each of the two diagnosis views and aluminum steps in one of the views for an optical depth reference. With this cap design, the tube is fully supported and constrained.

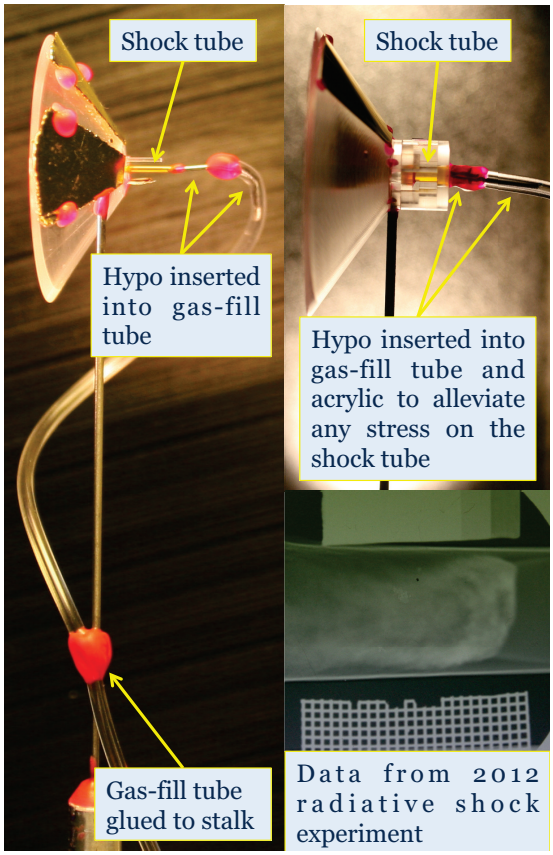

Figure 1. The target on the left is from our 2011 Radiative Shock experiment. The Tygon gas fill tube needed to be glued onto the stalk in such a way as to reduce the chances of damaging the polyimide shock tube. This same target was redesigned into the target depicted on the right. Here, the 2012 Radiative Shock target has the tube well supported and aligned to diagnostic viewing windows and fiducials. The bottom right figure is a radiograph from the 2012 radiative shock experiment. It shows how important the alignment of the shock tube is to obtaining quality data.

2. Integration of 3D Printing

Because of the benefits of designing targets using acrylic structures to constrain target components, we do all we can to utilize this design technique for all of our target builds. 3D printing technology has improved immensely in the past several years, therefore this became a natural progression for manufacturing target bodies, especially when the benefits of 3D printing include smaller time scales and larger quantities for a fraction of the cost. There was also the ever-present desire to create target designs that are free from the constraints inherent with

traditional machining. This freedom holds the possibility of breaking present boundaries in target design, which dictate any new physics born from such experiments. Like any new scientific essay, we needed to understand and learn how to work with new constraints that accompany new freedoms. Here we detail our unexpected challenges in this endeavor.

The 3D printer used for the targets and support equipment mentioned in this paper is the Viper. All of the details about making parts for our experiment will be specific to this device. The Viper 3D printer, among several others, is located at the University of Michigan's Medical Innovation Center. It uses Stereolithography (SLS) technology with a UV cured resin to create the parts. The process is as follows. A CAD model in the form of an .stl file is uploaded into the machine. The user then has several options as to how to orient the part for printing, where to position support scaffolding and where to print them on the plane of the platform. There are many subtleties to these options that will be described in detail below. The basic printing process has a stationary Neodymium-doped yttrium orthovanadate (Ny:YVO_4) laser positioned above the center of a one foot square platform. This platform sits within a vat of resin. At the start of a printing run the platform has a very thin layer of resin on top of it. Mirrors move to point the laser beam to different parts on this thin film of resin on top of the platform. The laser shoots a pulse and cures a tiny amount of the resin on top in the exact locations of the parts on the platform. This is the first layer of the fully formed part. The platform then moves 25 μm down, into the resin and the next layer is cured.

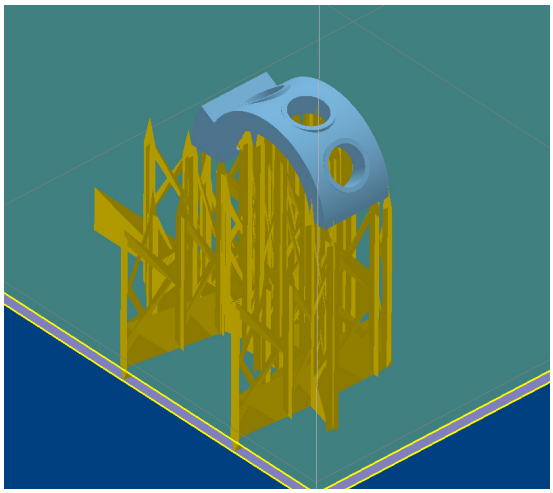

Figure 2. This is a screen shot of our 2013 Thomson Scattering Jet target and how the 3D printing software allows us to see how the part is oriented and the scaffolding that the Viper SLA will print to support the arch in the middle of the part. Here the user can adjust the scaffolding as desired to optimize the nominal design of the part.

The fully formed part will have scaffolding attached to the base of the part (Figure 2). This scaffolding supports the part on the platform and any features of the part that are not flat in the printing plane. If there are holes or arches or overhangs, this scaffolding will add support while the rest of the part is printed. It is intentionally brittle so it breaks easily from the platform and is easy to clean from the part. Figure 2 shows a screen shot of our 2013 Thomson Scattering Jet target that was 3D printed. We chose this specific orientation to print the part to maximize accuracy on particular features. The software then displays how the scaffolding will print out as well. The user may then have the option of modifying the part orientation and scaffolding, among other options.

Our first attempt at 3D printing using University of Michigan's Viper (SLA) was to print

out a proven target design. This target was for our 2012 Richtmyer-Meshkov campaign. The original target consisted of two parts that mated together in a unique configuration to tightly house a target package that when irradiated would create a Richtmyer-Meshkov instability. The original target, first fielded in 2011, was machined from polycarbonate so that the housing itself could also be directly ablated, as polycarbonate was the ablator for this physics package. This is an important detail because the 3D printed resin is very similar to the composition of acrylic. Therefore, directly ablating the 3D printed target would not be possible in this experiment, as will the case be for other target designs covered in this paper. The original design was then modified to add a hole on the ablator front of the 3D printed target. The addition of a layer of polycarbonate film was then added to the target package. A trivial modification when considering the greater than two weeks needed to machine the 2011 version of the targets through traditional methods is dramatically reduced to four hours of printing time. This is a winning trade off in cost. Machinist time alone would have been at least a magnitude higher in cost.

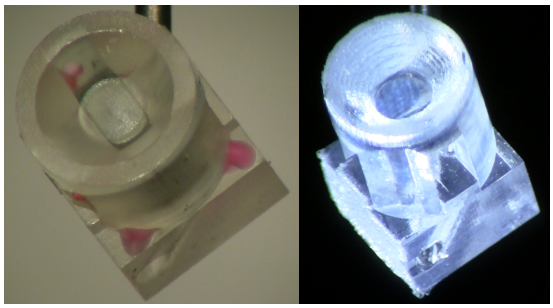

Figure 3. The target on the left is from our 2013 Richtmyer Meshkov experiment. It was machined from polycarbonate, the same material as necessary for our ablator. Therefore, the front of the target is machined down to a thin membrane. The stalk hole is drilled through to fix the angle and is shown here stalked. The target on the right is the 3D printed version. The front is hollow because the 3D printed material is nearly identical to acrylic. In this case the 3D printed cone cannot be part of the physics package and ablated directly. Therefore, a thin film of polycarbonate was inserted with the rest of the physics package to act as ablator. A small concession for the ability to obtain an entire campaign's worth of these parts within one day for for simply the cost of the resin used to make the parts. This is at least an order of magnitude less than the two weeks of a machinist's time to traditionally machine the parts.

To fully capitalize on the values of 3D printing, our next attempt at utilizing this service was with our June 2013 Titan Magnetized Plasma experiment at LLNL. With this experiment we gained the most experience in understanding the benefits and the true limitations of 3D printing with our specific printer, on the scale and holding the necessary tolerances of our parts. This experiment required no less than 160 targets. Along with all required targets, we also needed to construct a solenoid with special housing necessary to confine the epoxy surrounding the copper coils. This housing was not machinable through traditional methods without a considerable investment of time. To diagnose the magnetic field in the solenoid, B-dot probes would also need to be made. The targets, solenoid housing and B-dot probes for this experiment were drastically different in scale and use.

2.1. Resin

For this Titan experiment, the largest obstacle regarding the main target was that it was designed to be directly ablated by the laser to create the plasma jet. Pure acrylic would have been

acceptable, as it was used in the last iteration of this experiment. Unfortunately, the material used by our 3D printer is Accura 60, an UV-cured resin. Though the composition of the resin is very similar to acrylic, there is a trace amount of an element that acts as a catalyst to assist in hardening the resin to form 3D parts. This element is Antimony (Sb) and is high-Z (z = 51). According to the MSDS, there can be as much as 5 atom % of Sb. The resin was analyzed on a sample of cured resin and calculated to have atom % of the Sb $\sim$ 0.3 for that particular run.

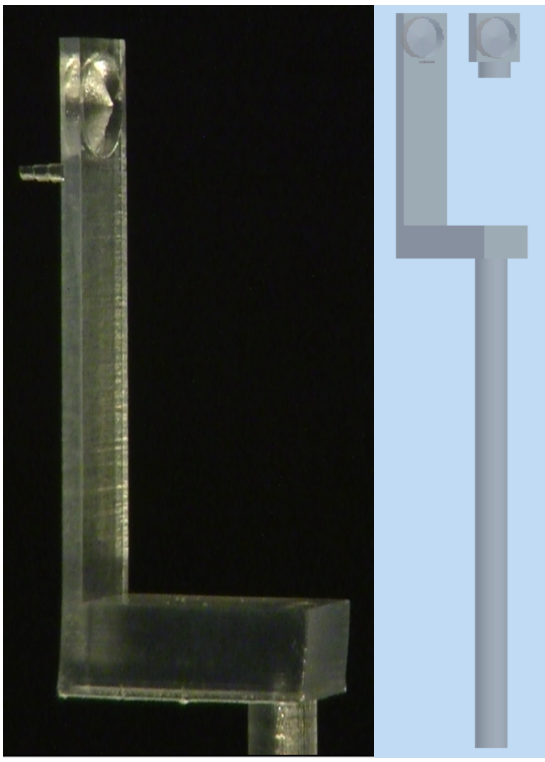

Figure 4. The left target is our 2013 Titan 3D printed Magnetized Plasmas jet target. The target and it's stalk are printed as one. On the right is a 3D model of how sample heads were printed for analysis. In the actual printing process, scaffolding is printed onto the base of the sample head to keep it in the same location as the 3D model. This allows us to accurately characterize the targets used in the experiment, as parts printed at different locations in different runs can have slight variations that on the scale of these targets may have an impact on the physics.

The target design was to consist of thin walled cones (Figure 4), whose wall thickness varied. We printed out cones whose nominal wall thickness was 50 μm, 100 μm and a third variety where the wall thickness started out at 50 μm and thickened axially to 100 μm. For the target with the varying wall thickness there was a step at the seam where the wall thickness abruptly went from the 50 μm to 100 μm.

Another advantage to 3D printing these targets, besides cost, was that the stalk could be printed as part of the target to make one complete piece (Figure 4). Therefore, no other assembly would be needed. Test pieces were printed along with the original run. The test heads were positioned in the same location as the head of the actual targets to maximize the chances of the test head being an exact duplicate of the actual targets. The right depiction in Figure 4 is a CAD drawing of how the test heads were printed out with the actual targets. The actual part was printed with scaffolding to hold the part in the position programmed into the CAD. Printing

test heads enabled us to easily place the physics portion of the targets into a μ-CT (MCT) scanner to fully characterize them, allowing us to analyze post-shot data more accurately.

The test heads were printed in this manner because there can be inconsistencies from part to part within one printing run. The platform that the parts are placed on is 12" x 12". But, there is an optimization zone within this platform that is the central 5" x 5" section of the platform. The reason for this is that the laser spot becomes an oblong circle when the mirrors reflects the laser at an angle to cure regions anywhere other than directly below the center of the laser. As the mirrors reflect the beam outward to print parts on the platform, the spot size takes on an elongated circular shape, much like the way headlights on a car will be oval-like on the road in front of you. The more at an angle they are pointed, the less round the light spot will be. We were attempting to mitigate this effect by printing out the test head as close to the true location of the actual target physics package as possible. The test heads were all MCT scanned to characterize the wall thickness that was printed out and shot during the experiment. The results showed that although we programmed the targets to have various wall thicknesses from 50 - 100 μm, they all tended to be $\sim$ 75 μm. Printed out, the cones did not differ much from one another regardless of what the nominal was. This was a bit discouraging.

2.2. Layer Correction

For this experiment, the shape of the cone was also important. Here, we began to understand the issue of layer correction in its entirety and how big of an impact it has on parts of this scale. This is the aspect of 3D printing that transforms it into an art and shows the importance of the human element to the entire processes.

Over-curing occurs because when the laser beam hits the resin, the energy of the laser spot emanates spherically. How much of the resin actually cures due to the laser spot hitting the top of the resin is a function of the viscosity. Though the laser spot size itself is small, $\sim$ 25 μm, the energy moves through the resin in 4π. The final volume that actually cures is $\sim$ 75 μm in diameter. This $\sim$ 75 μm is added on to all downward surfaces. Therefore, the resolution of parts cannot be determined by the machines laser spot size or how incremental the stage moves to print each level. These are figures that are quoted in each machine's literature, but are not a true representation of the resolution at which the device can actually print. Therefore, the user must be keenly aware how over-curing will effect certain surfaces of the part and make adjustments to the original CAD drawings or when programming the printer itself.

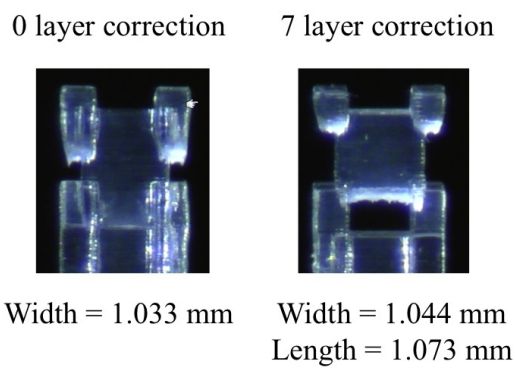

Figure 5. This slide shows a close-up of a 3D printed B-dot probe tip. Over curing effects all downward facing surfaces. In this case, the left part shows how over-curing caused the gap to become completely closed. Layer correction programs the 3D printer to not print a chosen number of layers. Therefore, the over-curing that does occur will form the part as intended.

In the specific case of these jet targets, where the bored out cone feature is circular, the true shape that is printed out, with no software manipulation, is more of an oval. The minor axis is in the vertical direction, making a circular hole more oval, as the layers on the top, downward facing arch of the opening, over-cures. For these targets this was a nontrivial issue because the region to be irradiated by the laser must be as uniform as possible. This means that we had to make the cone a larger diameter, so that even if from a wider view the cone was more oval than circular, within the region that is being irradiated by the laser in the experiment, it will appear as round as the laser spot. But, there was a limit to how large of a diameter we could have because the target had to fit in the slit of the solenoid.

One way to approach this problem is layer correction. This involves fooling the 3D printer into printing less layers than we would in a perfect system. The layer correction effects all downward facing surfaces within that part. For instance, if you program the machine not to print the first three layers, you essentially eliminate several tens of microns in over-cured material on every downward facing surface. This is illustrated in Figure 5. This slide compares between printing a part with no layer correction and one with 7-layer correction, the amount for this specific part that gave us the dimensions we needed to match the nominal.

The part shown in Figure 5 is the head of a B-dot probe in which the finished part, shown in Figure 6, will have 150 μm diameter magnetic wire wound around the central cube in three orthogonal directions.[2] To this end, we needed the center cube to be as cubic as possible, therefore the sides of the center cube needed to be as equivalent in their dimensions as possible so that when we wound the magnetic copper wire around the center cube the inside diameters of the loops would be as similar as possible. Adjusting the software on the printer so that it did not print the first seven layers, enabled us to get a final part with a center cube that was very close to nominal.

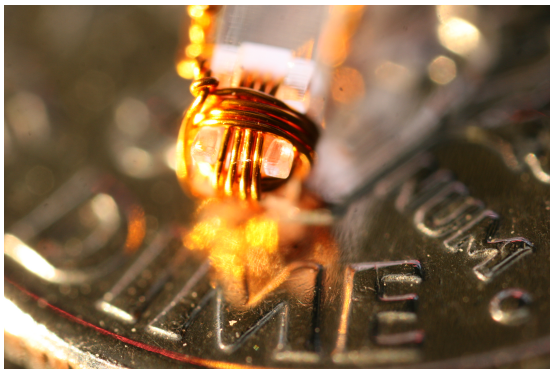

Figure 6. Here is a close-up of a 3D printed B-dot probe tip with magnetic copper wire wound in three orthogonal directions. This was used to characterize the magnetic field in the solenoid used in our 2013 magnetized plasma jet experiment (Figure 7).

Another way to approach the problem of over-curing is to simply modify the CAD file to have a larger opening to begin with. In essence, you could program the CAD model to have many of the same dimensions as the nominal part, but with a larger opening to take into account the printer's over-curing the top of the opening. We typically use this option for printing holes whose orientation are vertical, parallel to the printing direction. Recalling that over-curing occurs spherically, all outer surfaces, including inside edges of holes, will cure outward another ~ 50 μm horizontally beyond the nominal laser spot size. Modifying the CAD file to compensate for the over curing in downward facing surfaces does not normally save time in the overall process because you still must print out several test pieces and then go back and modify your CAD file until you gat the part in the correct dimensions. Simply having the machine omit layers is a

quicker turn around and less steps. Unfortunately, when making vertical holes there is no other alternative but to modify the CAD file and go through trial and error.

2.3. Solenoid Housing

For this same experiment, a solenoid was built to create a magnetic field around the plasma jet emanating from the ablated 3D printed cone target. The housing encapsulating the copper coils needed to be 3D printed because their shape was not feasible to machine in the traditional sense. This solenoid was fielded on Titan at LLNL for the plasma jet experiment aforementioned. The solenoid consisted of two copper coils welded together by a copper bridge that allowed for a $\sim$ 5 mm gap between the coils to position targets. Because of this bridge and the need for as much diagnostic viewing freedom as possible, the housing around the copper coils and connecting bridge had a very sophisticated design that was too labor intensive to be machined by traditional established methods. Our 3D printer worked very well for parts of this scale. The walls were made of several pieces that mated together to seal in the epoxy encapsulating the bridge and copper coils. The curves in the walls minimized the overall volume of the finished solenoid.

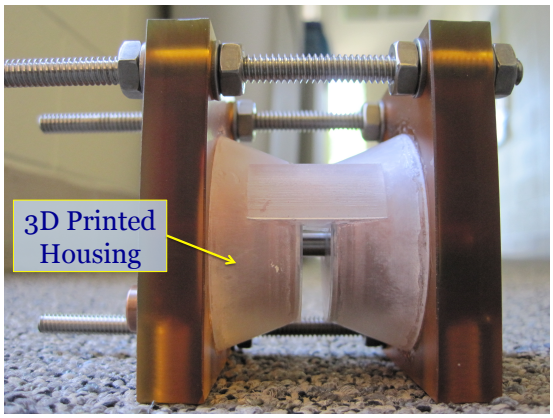

Figure 7. The solenoid pictured here was used to create a magnetic field for our 2013 Titan magnetized plasma jet experiment. The outer housing that enables the copper coils to be encapsulated in epoxy needed to be 3D printed because of its conical shape and bridge. This specialized housing maximized diagnostic views and was simply not reasonable to traditionally machine.

2.4. Combining 3D Printing and Traditional Machining

In July of 2013 using our Magneto-Inertial Fusion Electrical Discharge System (MIFEDS) [4] target design, we began to combine traditional machining with 3D printing. For MIFEDS targets, the challenge lies in creating stalks at stalk angles that simply cannot be traditionally machined. This target contained copper wire pulsed with a current, while three cones were ablated. The stalk of the MIFEDS is far more complicated than normal stalks because the stalk is fastened directly to the electronics that pulse current through the copper wire wound abound the target to create a magnetic field (Figure 8). Combining the MIFEDs and the target into one complete target, simplified alignment considerably. This simplification of having to align our ablated target and the MIFEDS coils saved us at least one shot on this shot day (Figure 9).

The conical portion of the target could not be printed along with the rest of the target body. Tiny cones had to be machined through traditional methods and glued onto the target. Firstly, we already knew from the Titan Plasma Jet targets (Figure 4) that we could not print a small circular opening. Also, the preceding experiment ablated acrylic. As mentioned with

Figure 8. This is an LLE MIFEDS coil. Here it can be seen how the MIFEDS, once wound with the copper coil, is attached to the electronics package.

the magnetized jet experiment, the high Z Sb in the cured resin would have not been consistent enough with past experiments. Therefore, analyzing data would have been difficult.

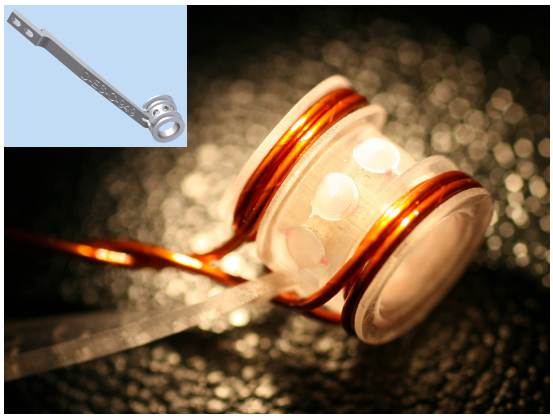

Figure 9. The inset target located in the upper left hand corner is a CAD model of the entire MIFEDS target before the cones are attached and copper wire is wound. A close-up of the finished target is center. Three traditionally machined cones of 2.5 mm OD are attached to the three bored holes in the 3D printed target and magnetic copper wire is wound on each side of the physics package to create a magnetic field when pulsed.

2.5. 3D Print Orientation to Mitigate Over-curing

Choosing a print orientation was very difficult with this target. For this experiment, the final orientation of the cones was extremely important. This target was particularly sensitive to alignment issues because the laser beams needed to hit the cones all at the same time, precisely on their apex's. Therefore, the cones had to be pointed radially inward within 10's of microns from nominal. This target was printed with the hollow of the cylindrical barrel orientated in the horizontal direction, with the center cone hole printed directly vertical (Figure 10). This enabled us to have the inset, where the coils would be wound, well positioned on both sides of the cone holes. Had we printed this target with the hollow of the barrel in the vertical direction then the edges of the inset, where the copper wire is wound, would be thicker due to over-curing, thus crowding the space where the wires were supposed to be placed. The target was precisely sized to minimize volume and avoid blocking beams while in the target chamber. Therefore, enlarging the target to compensate for thicker walls on the insets was not an option.

Within this Plasma Jet experiment day, Thomson scattering targets were shot as well. This target design was very similar to the MIFEDS target. It had three cones arranged in the same formation as the MIFEDS target, but there were no coils needed and the target could be stalked on a pin mount as our normal targets are. These targets were 3D printed in the same orientation as the jet target, with the center cone hole directly vertical (Figure 2). Before shooting the Thompson Scattering target it was micro-computerized tomography (MCT)

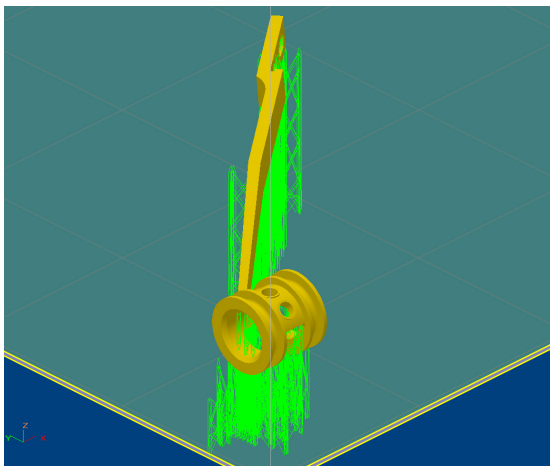

Figure 10. This is a screen shot of the print orientation of the MIFEDS plasma jet target. This orientation was chosen to print the insets, the ruts flanking the cone holes where the copper wire would be wound, as precisely as possible. It was important that the copper coils would be as close to nominal as possible so that when they were pulsed during the experiment the magnetic field bold be generated in the correct location.

scanned to characterize where the cone holes were with respect to the center axis of the arc (Figure 11). Analyzing slices showed that the cone holes were within a degree of nominal.

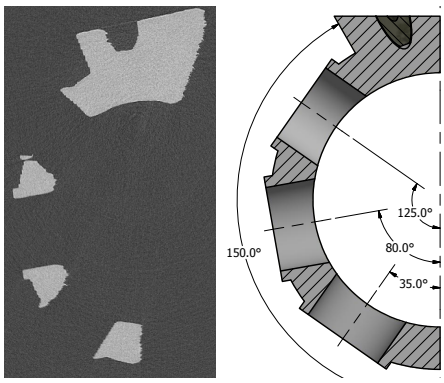

Figure 11. The left depiction is the slice of a MCT scanned Thomson Scattering target. The bored holes in which the cones would be attached measured to be less than one degree off radius from nominal.

2.6. Back Machining 3D printed Targets

In 2014 our X-ray fluorescent campaign using Trident Laser at LANL required 125 shots in short time scale. [3] This target design was quite similar to the Radiative Shock target described in the motivational section.It contained a tube that needed to be well aligned and at least one cone for shielding, though this particular design carried other complexities. For the experiment we needed to have the tube as straight as possible and exposed to as many degrees of diagnostic viewing as possible, in this case 300°. Two cones were required for shielding, one placed on both sides of the physics package. Lastly, the collet that the stalk is mounted into in the target

chamber was square. To capitalize on this square mounting system, we designed a square stalk with a square stalk hole. This square stalk hole was to be created within mortise and tenon joints mated together to constrain the rotation of the completed target. This would make target alignment trivial. Figure 12 shows how the two cones mated together at the mortise and tenon joint, using the square stalk to lock them into place. Within the cones themselves were counter bores. These were necessary to fit the tube into, as well as positioning a collimator and foils for the drive and probe beams.

With this double cone design, the 125 targets needed for the entire campaign means that 250 cones would need to be machined. Micro-machining this amount of cones, with the mortise and tenon joints and several different diameters of counter-bores in the time frame needed was unfeasible. Test 3D printed pieces from the CAD model of this target did not come out acceptably. Because the tube needed to fit snuggly into the cone's through-holes and line up precisely with the through-hole in the other mated cone in order to align with the tube. To this end, only one orientation would work, which was to print the cone with the large diameter flat on the platform and mating features facing up. Printed this way, the counter-bores did not have well enough defined surfaces to attach foils concentrically and over curing would cause the through-holes to be too small in diameter. Also, with this orientation the square stalk hole that sits perpendicular to the target axis, would not be the correct dimensions because of over-curing.

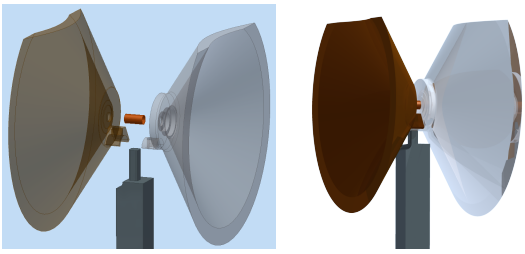

Figure 12. This is our 2014 Trident X-ray Fluorescence target. The CAD rendering on the left is a blowout of the target and details the mating parts. The rendering on the right shows the target fully assembled.

For these cones we chose to utilize 3D printing to print out rough blanks of the cones. This would take advantage of 3D printing by forming parts that allowed loose tolerances and demanded little skill, such as the cones that need only provide a minimum amount of shielding and beam clearance. Printing out blank cones alleviated the need for precious machine time that would otherwise be wasted simply hogging out material when turning a solid cylindrical piece of sock into a cone on a lathe. Turning parts like these would tie up a machine for several days and occupy a skilled machinist's time unnecessarily. Ultimately, we chose to 3D print the blanks and only invest our machinist's time on the fine details of the cones. The part was printed with the larger diameter facing up, while printing extra material on the back of the cone to be able to back machine the mortise and tenon joints and mating features, as well as all of the counter-bores. With this compromise we were able to take advantage of the best aspects of both 3D printing and traditional machining. Figure 14 shows a completed target in a jig, where the mating parts and square stalk allowed us to build the entire target by hand, with no special equipment.

3. Conclusion

3D printing technology has advanced in sophistication over the past several years. With evermore complex target designs it has become an important endeavor to investigate how best to utilize 3D printing on a millimeter scale so that the quality of targets continues to be high, yet allow

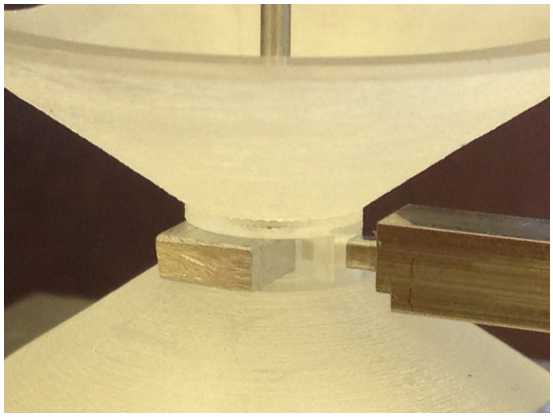

Figure 13. This is a close-up view of our 2014 Trident X-ray Fluorescence target showing how the two cones mated together. A square stalk with square stalk hole was used to easily fix orientation of the target once placed in the target chamber. A spacer sandwiched between cones and a rod threaded through both cones constrained these components during the build.

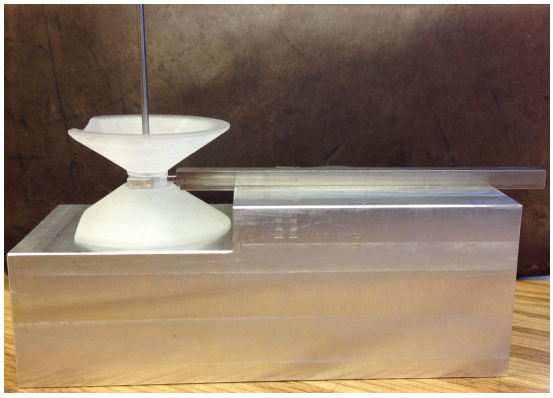

Figure 14. Along with the spacer and rod used to constrain the cones our 2014 Trident X-ray Fluorescence target, shown close-up in Figure 13, a simple jig supported the stalk and constrained the rod that threaded through both cones and into base of the jig. It is jigs such as these that allow us to construct targets with little or no specialized equipment.

us to create designs that traditional machining could not otherwise accomplish. For the scale of targets that are used in our experiments, 3D printing alone was not often feasible. But, in navigating through the constraints that are inherent in 3D printing parts of this size and combining traditional machining techniques, 3D printing provides valuable benefits to target fabrication through its cost effectiveness and shorter manufacturing time scales.

Acknowledgments
This work is funded by the U.S. Department of Energy, through the NNSA-DS and SC-OFES Joint Program in High-Energy-Density Laboratory Plasmas, grant number DE-NA0001840, and the National Laser User Facility Program, grant number DE-NA0000850, and through the Laboratory for Laser Energetics, University of Rochester by the NNSA/OICF under Cooperative Agreement No. DE-FC52-08NA28302.

[1] Klein S, *et al*, Innovations in target fabrication techniques at the University of Michigan 2013 *FST* **63** 2 305-12

[2] Klein S R, Manuel M J-E, Pollock B B, Gillespie R S, Deininger M, Kuranz C C, Keiter P A and Drake R P Construction of a solenoid used on a magnetized plasma experiment 2014 *Rev. Sci. Instrum.* **85**

[3] MacDonald M J, *et al* Demonstration of x-ray fluorescence imaging of a high-energy-density plasma 2014 *Rev. Sci. Instrum.* **85**

[4] C. K. Li, *et al* Magneto-Inertial Fusion...Enlisting Magnetic Fields for Improved Laser-Fusion Implosions 2006 *Rev. Sci. Instrum.* **77** 10E725